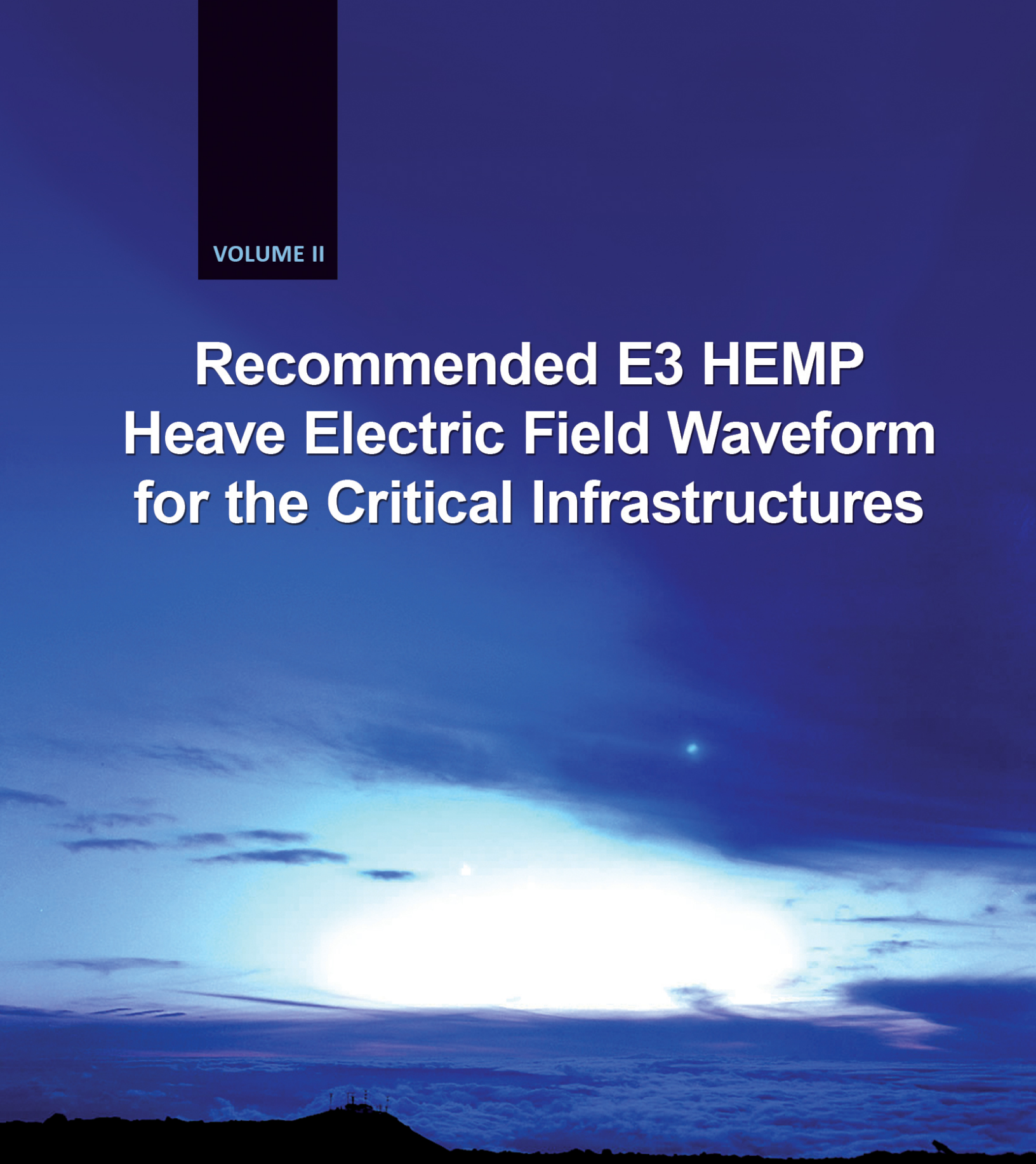
VOLUME II

Recommended E3 HEMP Heave Electric Field Waveform for the Critical Infrastructures



JULY 2017

Report of the Commission to Assess the Threat to the United States from Electromagnetic Pulse (EMP) Attack

Recommended E3 HEMP Heave Electric Field Waveform for the Critical Infrastructures

July 2017

REPORT OF THE COMMISSION TO ASSESS THE THREAT TO THE UNITED STATES FROM ELECTROMAGNETIC PULSE (EMP) ATTACK

The cover photo depicts Fishbowl Starfish Prime at 0 to 15 seconds from Maui Station in July 1962, courtesy of Los Alamos National Laboratory.

This report is a product of the Commission to Assess the Threat to the United States from Electromagnetic Pulse (EMP) Attack. The Commission was established by Congress in the FY2001 National Defense Authorization Act, Title XIV, and was continued per the FY2016 National Defense Authorization Act, Section 1089.

The Commission completed its information-gathering in June 2017. The report was cleared for open publication by the DoD Office of Prepublication and Security Review on April 9, 2018.

This report is unclassified and cleared for public release.

TABLE OF CONTENTS

EXECUTIVE SUMMARY 1

1 INTRODUCTION 2

2 GROUND CONDUCTIVITY PROFILES 7

3 SOVIET E3 HEMP MEASUREMENTS 9
Test Parameters 9
Scaling of the Results 19
Latitude Scaling 19
Pattern Scaling 20

4 CONCLUSIONS 24

LIST OF FIGURES

Figure 1 Parts of HEMP. E3 HEMP heave is roughly described by the second peak in the MHD signal. [SOURCE: Meta R-321] 3

Figure 2 Diagram of the E3 HEMP heave effect. [SOURCE: Meta R-321] 4

Figure 3 Sample normalized yield variation for maximum E field for heave for burst heights between 130 and 170 km and for a fixed Earth conductivity profile. [SOURCE: Meta R-321] 5

Figure 4 Sample normalized HOB variation for maximum peak E field for heave for an intermediate yield weapon and for a fixed Earth conductivity profile. [SOURCE: Meta R-321] 6

Figure 5 Ground conductivity depth profile for three ground profiles. 7

Figure 6 Ground profile B-to-E conversion in the frequency domain for three cases. 8

Figure 7 Simulation of the Soviet tests showing B field peaks and field directions,150 km test (R2). 10

Figure 8 Simulation of the Soviet tests showing B field peaks and field directions, 300 km test (R1). 11

Figure 9 Measured B fields at N1, 150 km test 12

Figure 10 Measured B fields at N2, 150 km test 12

Figure 11 Measured B fields at N3, 150 km test 13

Figure 12 Measured B fields at N1, 300 km test 13

Figure 13 Measured B fields at N2, 300 km test 14

Figure 14 Measured B fields at N3, 300 km test 14

Figure 15 E field amplitudes for four ground profiles, at N1, 150 km test 16

Figure 16 E field amplitudes for four ground profiles, at N2, 150 km test 16

Figure 17 E field amplitudes for four ground profiles, at N3, 150 km test 17

Figure 18 E field amplitudes for four ground profiles, at N1, 300 km test 17

Figure 19 E field amplitudes for four ground profiles, at N2, 300 km test 18

Figure 20 E field amplitudes for four ground profiles, at N3, 300 km test 18

Figure 21 Geomagnetic latitude variation, for a 150 km burst, over the U.S. The black line is at 48.92°, which is the computed geomagnetic latitude for the 150 km Soviet test 20

Figure 22 Normalized simulated B field peaks versus ground range for the 150 km test. The black dot shows the simulated results for the N3 point 21

Figure 23 Normalized simulated B field peaks versus ground range for the 300 km test. The black dot shows the simulated results for the N3 point 22

Figure 24 E field waveform shape, using the measured N1 waveform from the 150 km burst height 24

Figure 25 Normalized E peak contour pattern from the 150 km burst case 25

LIST OF TABLES

Table 1 Geometry for the Soviet High-Altitude Tests. 9
Table 2 Peaks of the Soviet measurement waveforms. (The E field is for the 10^{-3} S/m ground.) 15
Table 3 Geomagnetic latitude scaling of the Soviet measurements. 21
Table 4 Pattern (observer position) scaling of the Soviet measurements. 22
Table 5 Scaling of the Soviet Measurements. 24

ACRONYMS AND ABBREVIATIONS

B	magnetic field
CONUS	continental United States
DoD	Department of Defense
E	electric field
EMP	electromagnetic pulse
EPRI	Electric Power Research Institute
FERC	Federal Energy Regulatory Commission
GMD	geomagnetic disturbance
HEMP	high-altitude electromagnetic pulse
HOB	height of burst
km	kilometer
m	meter
MHD	magnetohydrodynamic
min	minute
NERC	North American Electric Reliability Corporation
nT	nanotesla
S/m	siemens/m
UV	ultraviolet
V	Volt

PREFACE

This EMP Commission Report, utilizing unclassified data from Soviet-era nuclear tests, establishes that recent estimates by the Electric Power Research Institute (EPRI) and others that the low-frequency component of nuclear high-altitude EMP (E3 HEMP) are too low by at least a factor of 3. Moreover, this assessment disproves another claim--often made by the U.S. Federal Energy Regulatory Commission (FERC), the North American Electric Reliability Corporation (NERC), EPRI and others—that the FERC-NERC Standard for solar storm protection against geo-magnetic disturbances (8 volts/kilometer, V/km) will also protect against nuclear E3 HEMP. A realistic unclassified peak level for E3 HEMP would be 85 V/km for CONUS as described in this report. New studies by EPRI and others are unnecessary since the Department of Defense has invested decades producing accurate assessments of the EMP threat environment and of technologies and techniques for cost-effective protection against EMP. The best solution is for DoD to share this information with industry to support near-term protection of electric grids and other national critical infrastructures that are vital both for DoD to perform its missions and for the survival of the American people.

EXECUTIVE SUMMARY

As described in this report, there is a need to have bounding information for the late-time (E3) high-altitude electromagnetic pulse (HEMP) threat waveform and a ground pattern to study the impact of these types of electromagnetic fields on long lines associated with the critical infrastructures. It is important that this waveform be readily available and useful for those working in the commercial sectors.

While the military has developed worst-case HEMP waveforms (E1, E2, and E3) for its purposes, these are not available for commercial use. Therefore, in this report openly available E3 HEMP measurements are evaluated from two high-altitude nuclear tests performed by the Soviet Union in 1962. Using these data waveforms and an understanding of the scaling relationships for the E3 HEMP heave phenomenon, bounding waveforms for commercial applications were developed.

Since the measured quantities during these tests were the magnetic fields, it is possible to compute the electric fields assuming ground conductivity profiles that produce significant levels. There are other profiles that would compute even higher electric fields, but some of these profiles do not cover a very large area of the Earth.

After computing the electric fields using the Soviet measurements, the results were scaled to account for the fact that their measurement locations were not at the optimum points on the ground to capture the maximum peak fields. Through this process, it was determined that the scaled maximum peak E3 HEMP heave field would have been 66 volts per kilometer (V/km) for the magnetic latitude of the Soviet tests.

As the E3 HEMP heave field also increases for burst points closer to the geomagnetic equator, the measured results were also evaluated for this parameter. This scaling increases the maximum peak electric field up to 85 V/km for locations in the southern part of the continental U.S., and 102 V/km for locations nearer to the geomagnetic equator, as in Hawaii. The levels in Alaska would be lower at an estimated peak value of 38 V/km (see Table 5 for information dealing with this scaling process).

It is noted that this report does not claim that the values provided here are absolute worst-case field levels, but rather these peak levels are estimated based directly on measurements made during Soviet high-altitude nuclear testing.

1 INTRODUCTION

Over many years beginning in the 1980s, the U.S. has worked to establish the peak field levels, ground patterns of the heave portion of the late-time E3 HEMP fields as shown in Figure 1, and from these to build useful models.[1,2] In the summer of 1994, Soviet scientists attending the European Electromagnetics (EUROEM) Symposium in Bordeaux, France, presented several papers indicating their understanding of the different types of EMP including the high-altitude electromagnetic pulse (HEMP). One of the most interesting developments of that conference was that these presentations summarized the Soviet high-altitude electromagnetic test results and indicated that the most important aspects of the effects they observed were caused by the "long tail" of the HEMP.[3] In later publications, they indicated that the long tail referred to the late-time HEMP, or the E3 HEMP magnetohydrodynamic (MHD)-EMP heave signal, and later provided detailed technical information indicating that the failure of one long-haul communications line was due to this portion of the HEMP.[4] Three other references dealing with E3 HEMP (MHD-EMP) were published by Soviet scientists in this time frame presumably due to their interest in understanding the failures of commercial long line systems during their 1962 high-altitude nuclear testing program over Kazakhstan.[5,6,7]

Later in the early 2000s, Soviet scientists provided the EMP Commission with a memo that illustrated their magnetic field measurements of the E3 HEMP heave signals at three locations during two of their high-altitude nuclear tests over Kazakhstan in 1962.[8] Because the Soviets tested over land instead of over ocean, as did the U.S., several long line systems were affected by the E3 HEMP fields. In addition, measurements of the magnetic fields were made at several locations on the ground at various ranges from the surface zero (the point directly underneath the high-altitude burst).

---

1 J. Gilbert, J. Kappenman, W. Radasky and E. Savage, "The Late-Time (E3) High-Altitude Electromagnetic Pulse (HEMP) and Its Impact on the U.S. Power Grid," Meta R-321, January 2010.

2 J.L. Gilbert, W.A. Radasky, K.S. Smith, K. Mallen, M.L. Sloan, J.R. Thompson, C.S. Kueny and E. Savage, "HEMPTAPS/HEMP-PC Audit Report." Meta R-131, December 1999; DTRA-TR-00-1, April 2002.

3 V.M. Loborev, "Up to Date State of the NEMP Problems and Topical Research Directions," Proceedings of the European Electromagnetics International Symposium -- EUROEM 94, June 1994, pp. 15-21.

4 V.N. Greetsai, A.H. Kozlovsky, V.M. Kuvshinnikov, V.M. Loborev, Y.V. Parfenov, O.A. Tarasov and L.N. Zdoukhov, "Response of Long Lines to Nuclear High-Altitude Nuclear Pulse (HEMP)," IEEE Transactions on EMC, Vol. 40, Issue 4, 1998, pp. 348-354.

5 V.N. Greetsai, V.M. Kondratiev, and E.L. Stupitsky, "Numerical Modelling of the Processes of High-Altitude Nuclear Explosion MDH-EMP Formation and Propagation," Roma International Symposium on EMC, September 1996, pp. 769-771.

6 "The Physics of Nuclear Explosions," Ministry of Defense of the Russian Federation, Central Institute of Physics and Technology, Volumes 1 and 2, ISBN 5-02-015124-6, 1997. MHD-EMP topics are found in Sections 13.5 and 13.6.3.

7 V.M. Kondratiev and V.V. Sokovikh, "Redetermination of MHD-EMP Amplitude Characteristics and Spatial Distribution on the Ground Surface," Roma International Symposium on EMC, September 1998, pp. 129-132.

8 "Characteristics of magnetic signals detected on the ground during the Soviet nuclear high-altitude explosions," memorandum provided by Soviet scientists, February 2003.

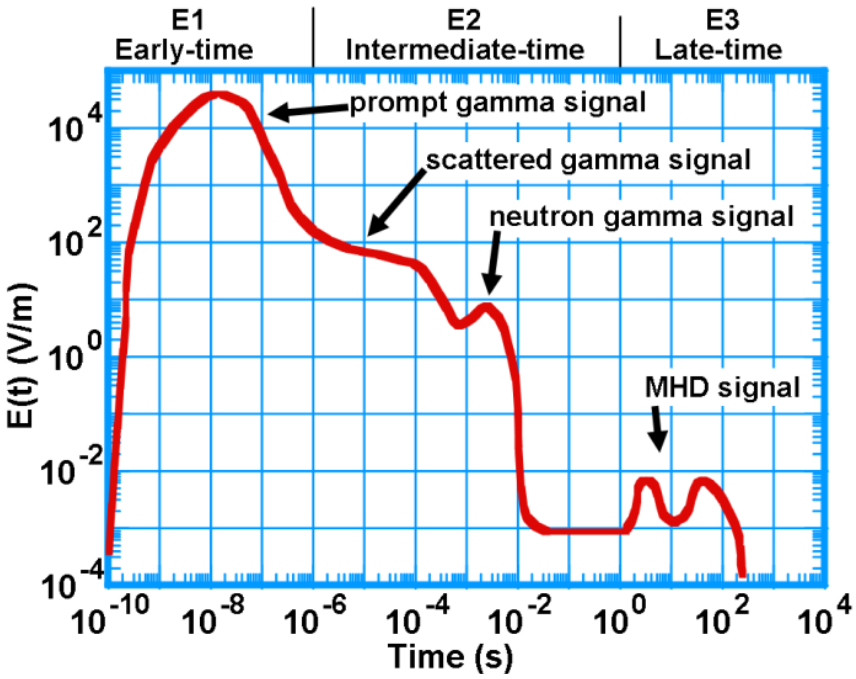


Figure 1 Parts of HEMP. E3 HEMP heave is roughly described by the second peak in the MHD signal. [SOURCE: Meta R-321]

In this report, the Soviet magnetic field data is reviewed, and through the use of several different ground conductivity profiles for locations in the U.S., the electric fields at the Earth's surface that could be induced are calculated. The magnetic fields are created by the nuclear detonation and the electric fields are induced in the earth and vary due to the particular deep conductivity profiles in the Earth. In addition, the magnetic fields (and electric fields) were also scaled to account for the fact that the Soviet measurements were not at the optimum ground locations to obtain the maximum peak fields on the ground. Finally, the increases in peak fields that would occur due to the well understood scaling of E3 HEMP with magnetic latitude were estimated, as the latitude of the Soviet tests were not at the bounding locations on the Earth.

The objective of this report is to determine from open source information how high the electric fields could be at latitudes of interest for the United States. In addition, a ground pattern and typical normalized electric field waveform is estimated that could be used for studies to determine the levels of quasi-DC currents that could be induced in long-line systems such as the bulk power system.

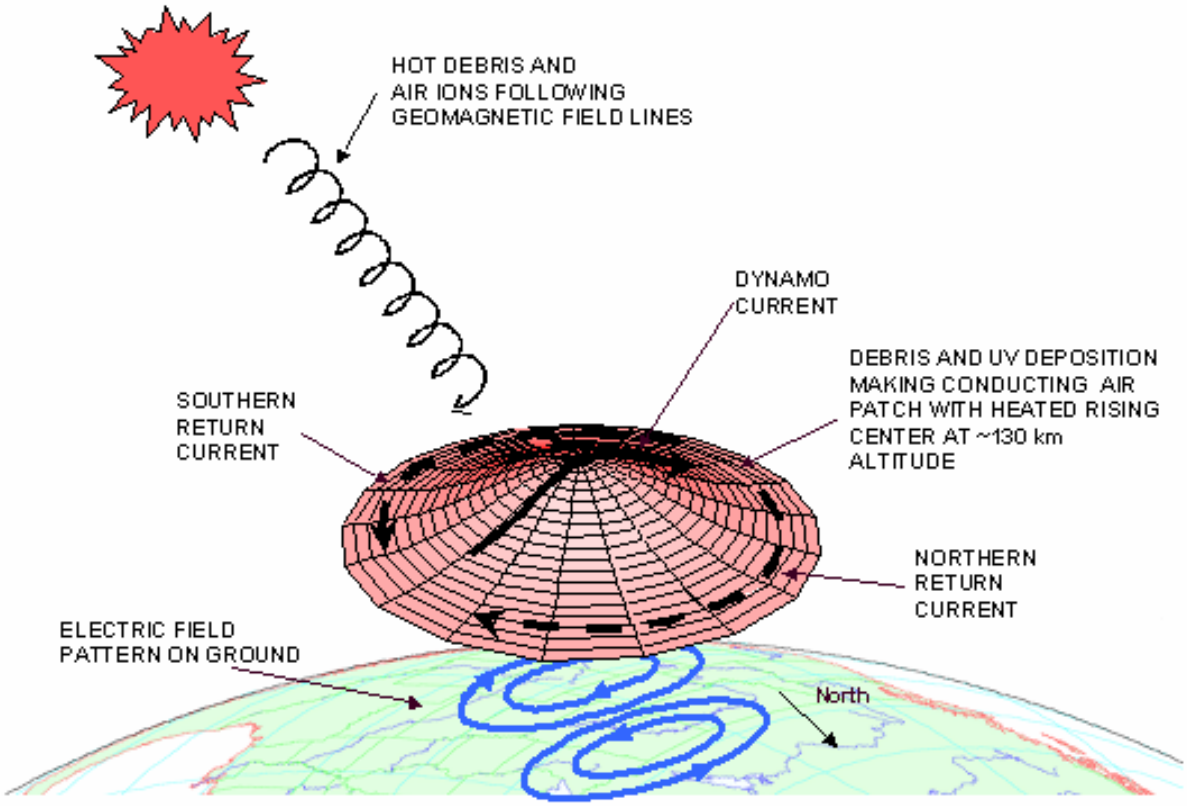


Figure 2 Diagram of the E3 HEMP heave effect. [SOURCE: Meta R-321]

This report does not claim that the values suggested here are absolute worst-case field levels, but rather these peak levels are estimated based directly on measurements made during high-altitude nuclear testing.

Figure 2 represents the E3 HEMP heave generation process. Hot ionized debris streaming downward away from the burst is directed preferentially along the geomagnetic field lines. As the debris and ultraviolet (UV) radiation from the burst reach altitudes where the atmosphere becomes dense enough, they heat up a “patch” of the atmosphere, and also add ionization to the background ionization already present in the ionosphere. The heat causes expansion, and the ionized region rises due to buoyancy. The Lorentz force on the ions and free electrons moving upward in the Earth’s geomagnetic field leads to east-west dynamo currents, with return currents completing the current flow on the north and south side. These currents induce image currents, with the associated electric fields, in the conductivity of the Earth below. Associated with this are magnetic (B) fields. The levels of the generated E fields are dependent on the actual ground conductivity to great depths of the Earth below the heaving patch, while the associated B field perturbations are approximately independent of the ground profile. For

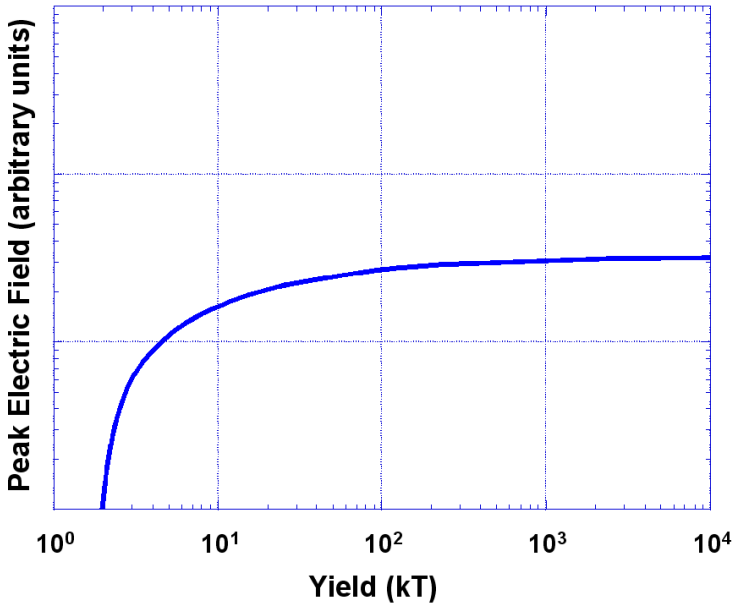


Figure 3 Sample normalized yield variation for maximum E field for heave for burst heights between 130 and 170 km and for a fixed Earth conductivity profile. [SOURCE: Meta R-321].

this reason, the measured B fields on the Earth's surface can be considered to be the principal E3 HEMP heave environment.

It is noted that there is a second mechanism that creates E3 HEMP fields on the ground called "Blast Wave", but while it also can produce significant B fields, the maximum fields are found thousands of kilometers away from ground zero. For this reason, the Blast Wave phenomenon is not considered in this report.

The E3 HEMP heave B field perturbation on the ground depends on many parameters, such as:

1. Burst parameters: The characteristics of the burst are important. Of primary importance is the burst yield—bigger bombs would tend to have more debris coming down and generating the E3 HEMP heave signal. Figure 3 shows a sample of E3 HEMP heave variation with yield. This yield dependence can vary with the burst height. In addition, the area of coverage for the peak field tends to be larger for larger yields.
2. Burst location: The burst location has two important effects. First, the height of burst (HOB) is important for E3 HEMP heave, as it is for other HEMP phenomena. The precise interaction with the atmosphere depends on how high the burst is above the atmosphere. Also, the higher the burst, the farther north (for northern hemisphere bursts) the heated patch is found, as it needs to travel a further distance on the tilted

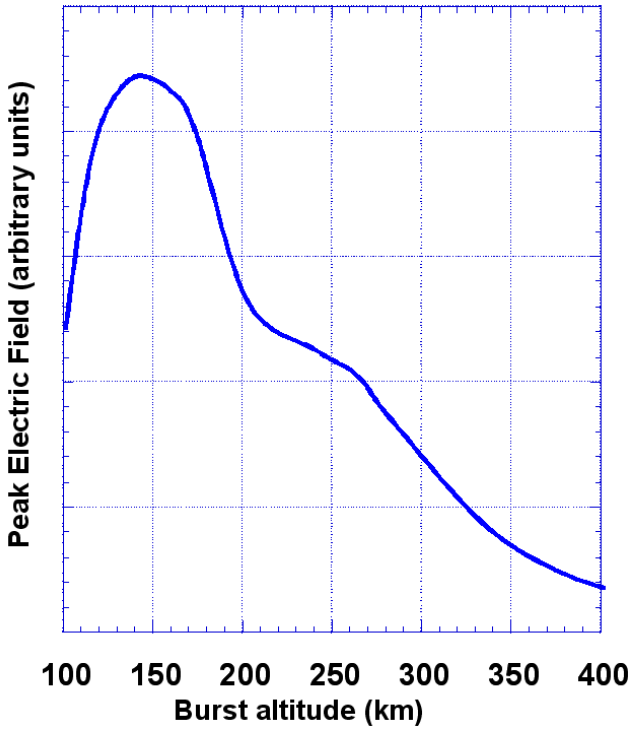


Figure 4 Sample normalized HOB variation for maximum peak E field for heave for an intermediate yield weapon and for a fixed Earth conductivity profile. [SOURCE: Meta R-321].

geomagnetic field lines. Figure 4 shows a sample of HOB variation for a fixed yield and ground conductivity profile. The other important location effect is the local geomagnetic field, which is represented by the value of geomagnetic latitude. One effect is that E3 HEMP heave gets weaker as the burst gets closer toward the (geomagnetic) poles, because the geomagnetic field becomes less horizontal, and there is less east-west deflection of the rising hot ions. (The geomagnetic latitude also affects the tilt of the path that the debris follows downward from the burst.)

3. Observer location: As seen in Figure 2, there is a 2-loop pattern of ground fields. The magnitude of the ground fields decreases with distance from the point directly below the patch. Examples of ground patterns are provided later in this report.
4. Burst time of day: Here the important factor is the “atmosphere”, basically the state of the ionosphere, which can vary significantly. Depending on the burst time, the day of the year, and the location, the burst may be in “night” or “day”. Sun exposure enhances the ionization of the ionosphere. For the E3 HEMP Blast Wave (the early-time portion of the E3 HEMP, which is not the subject of this report) the enhancement due to the “daytime” conditions depresses the E3 HEMP Blast Wave field, while for E3 HEMP heave there is an enhancement of the fields.

2 GROUND CONDUCTIVITY PROFILES

The E3 HEMP signal of concern in this report is the induced horizontal electric (E) field, as this field can effectively couple to long power and communications lines and induce quasi-dc currents in these systems. This coupling process has been discussed in several references including one that deals with geomagnetic disturbances (GMDs); GMD electric fields are similar in their time and frequency content to the electric fields produced by the E3 HEMP heave.[9] These E fields are produced by the presence of the conductivity depth profile in the Earth itself. For E3 HEMP heave it is the conductivity down to great depths (400-700 km) below the Earth's surface that determines the electric field. The E3 HEMP generation process begins with magnetic field (B) perturbations (relative to the geomagnetic field created by the Earth's core), and at the Earth's surface these B fields are little affected by the ground conductivity profile. Thus both calculations and measurements for actual nuclear tests typically begin with the B fields, and then E fields can be calculated for any assumed ground conductivity profile. While the induced peak E field is strongly related to the time derivative (dB/dt) of the horizontal B field, these calculations use the full Maxwell's Equations to determine the electric fields. The resulting E field is also horizontally oriented. The calculation of E from B must be done in terms of vector components—a B field in one horizontal direction creates an E field that is perpendicular to it under an assumed one-dimensional approximation for the local Earth conductivity profile.

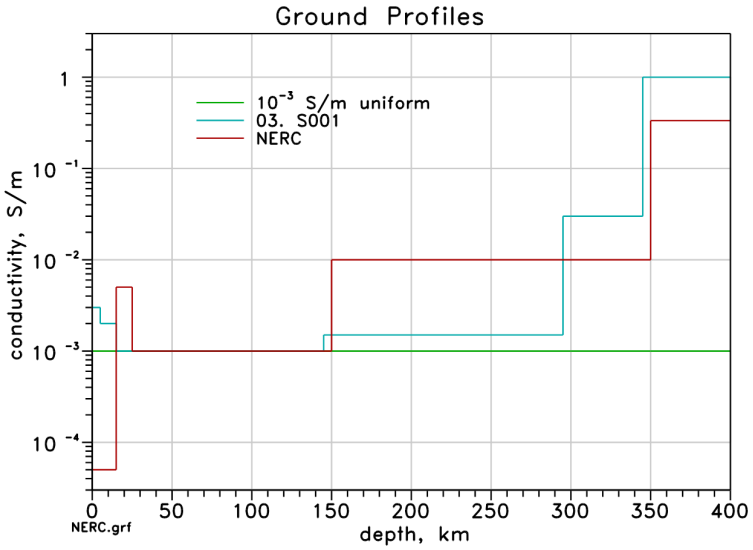


Figure 5 Ground conductivity depth profile for three ground profiles.

Figure 5 shows three ground profiles of ground conductivity with depth used in this report. The NERC profile (red line) has four layers of various conductivity levels, ending at a high

[9] W.A. Radasky, "Overview of the Impact of Intense Geomagnetic Storms on the U.S. High Voltage Power Grid," IEEE Electromagnetic Compatibility Symposium, Long Beach, California, 15-19 August 2011, pp. 300-305.

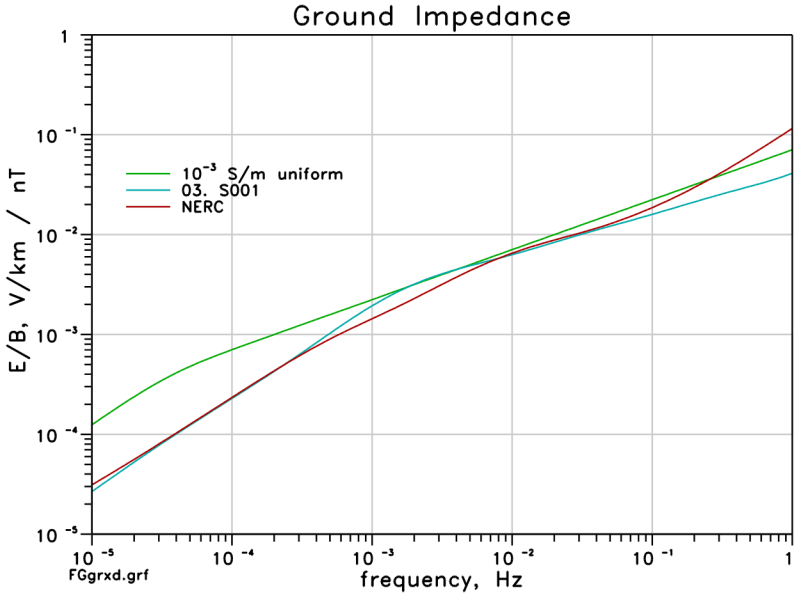


Figure 6 Ground profile B-to-E conversion in the frequency domain for three cases.

conductivity level that continues downward at its last value.[10] The E3 HEMP heave signals (due to their low frequency content) can penetrate through the upper layers of the Earth but will not penetrate much deeper when they encounter a high conductivity lower level (due to the pressures and temperatures found in the upper mantle of the Earth). The blue line is another set of ground conductivity data applicable to eastern Canada developed by Metatech from geological data. The impedance curve developed from this conductivity profile is seen to be very similar to the NERC curve in Figure 6. The third profile shown (in green) has a uniform conductivity of 10^{-3} S/m, which is used for simplicity in the E3 HEMP heave simulations shown later in this report.

Figure 6 shows the resulting impedance (conversion of B to E) in the frequency domain. There are many ways to deal with these types of impedance curves relating E to B, although the technique used by the authors allows calculations of E from B in the time domain without converting to the frequency domain.[11] This has advantages for performing real-time computations when measuring geomagnetic storm disturbances. All three curves are reasonably close together for the important frequency range of 1 to 100 mHz, as this is the frequency range of typical E3 HEMP B-field disturbances.

---

10 "Transmission System Planned Performance for Geomagnetic Disturbance Events", TPL-007-1, available at https://bit.ly/2GQpQF1

11 J.L. Gilbert, W.A. Radasky and E.B. Savage, "A Technique for Calculating the Currents Induced by Geomagnetic Storms on Large High Voltage Power Grids," IEEE EMC Symposium, Pittsburgh, August 2012, pp. 323-328.

3 SOVIET E3 HEMP MEASUREMENTS

Toward the end of the development of the E3 HEMP computational models in the U.S., a paper that reported measurements made by the Soviet Union during two of their high-altitude nuclear tests in 1962 was provided to us through the U.S. Congressional EMP Commission by Soviet scientists.[12] This was high quality data, in that measurements were made at three fixed locations (designated N1, N2, and N3 by the Soviets as shown in Table 1 and Figure 7), and the B field measurements were provided for two horizontal vector components. There is some uncertainty concerning the precision of the test and measurement locations; however, the data provided greatly increased the information describing the E3 HEMP heave signal. High-altitude nuclear tests were performed by the U.S. mainly over the Pacific Ocean, and the locations for measuring the magnetic fields were not as diverse as for the Soviet measurements.

TEST PARAMETERS

The Soviet tests were reported to be at burst heights of 150 and 300 km altitudes, for the same device design with an estimated yield of 300 kT. The precise geometry (burst and observer locations) is not known, as there was some ambiguity in the data provided. The Soviet measurement paper does give range values (burst to observer distances) for all six measurements (three from each test), and these same values appear elsewhere in a consistent manner. (The Soviets tended to use the slant range from the burst to the ground location, not the ground range, but the ground range is easily calculated from the burst height.) A set of locations was used that are consistent with these values in the following discussions, using the understanding of the variation of the fields with location. These burst and observer locations are given in Table 1.

Table 1 Geometry for the Soviet High-Altitude Tests.

Test Locations			
Type	Position	Latitude (N)	Longitude (E)
Bursts	R1, 300 km	47.6°	64.9°
	R2, 150 km	47.0°	68.0°
Observers	N1	47.9°	67.4°
	N2	47.1°	70.6°
	N3	45.9°	72.1°

[12] "Characteristics of magnetic signals detected on the ground during the Soviet nuclear high-altitude explosions," memorandum provided by Soviet scientists, February 2003.

Using the simulation code in Meta R-321, the B field peak values were calculated for the two burst heights. The data is shown in Figure 7 for the 150 km burst height (R1) and in Figure 8 for 300 km (R2).[13] (The 300 km test was actually performed 6 days before the 150 km test, but the lower altitude case was described first). The peak contours are identified by their color, and the B field directions at the time of the peak are shown by the arrows. The burst and observer points are marked on the displays. Normalized results are shown in these figures as a nominal contour plot is desired to be used later in this report as a standard contour profile.

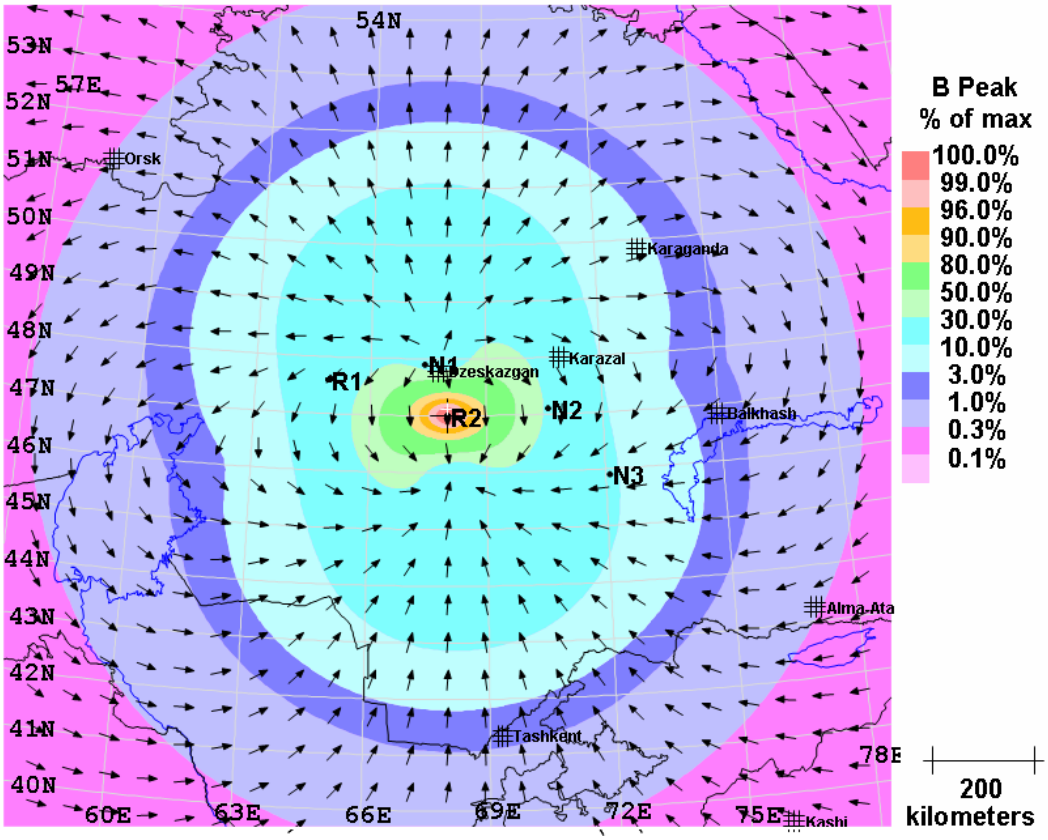


Figure 7 Simulation of the Soviet tests showing B field peaks and field directions,150 km test (R2).

[13] J.L. Gilbert, W.A. Radasky, K.S. Smith, K. Mallen, M.L. Sloan, J.R. Thompson, C.S. Kueny and E. Savage, "HEMPTAPS/HEMP-PC Audit Report." Meta R-131, December 1999; DTRA-TR-00-1, April 2002.

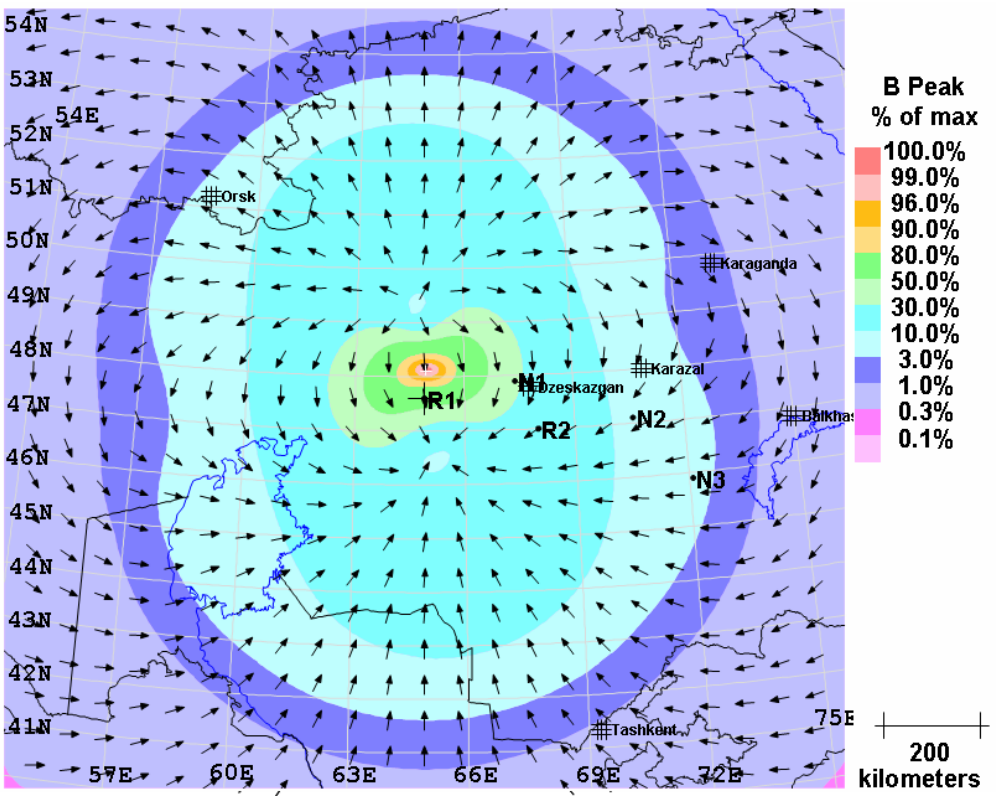


Figure 8 Simulation of the Soviet tests showing B field peaks and field directions, 300 km test (R1).

The next set of figures shows the measured B field time waveforms. The three lines are the north and west components, and the resulting magnitude. For the 150 km burst height case, shown in Figure 9 to Figure 11, the waveforms are all relatively wide in pulse width (the N1 case waveform has not returned to zero at the end of the 100-second window of the measurements). The peak occurs between times of 35 to 70 seconds. Figure 7 shows that N1 is close to the northern area of the two electric field depression points (the locations around which the two loops of E field circulate, as seen earlier in Figure 2) for this case. Here the time waveform may be complicated due to some shifting with time of the field depression point position. For the 300 km burst height waveforms, Figure 12 to Figure 14, the signals are faster, especially for N1. As noted, faster rising waveforms for the B fields enhance the E fields, because the impedance of the Earth behaves as $f^{1/2}$ (f = frequency) as shown in Figure 6.

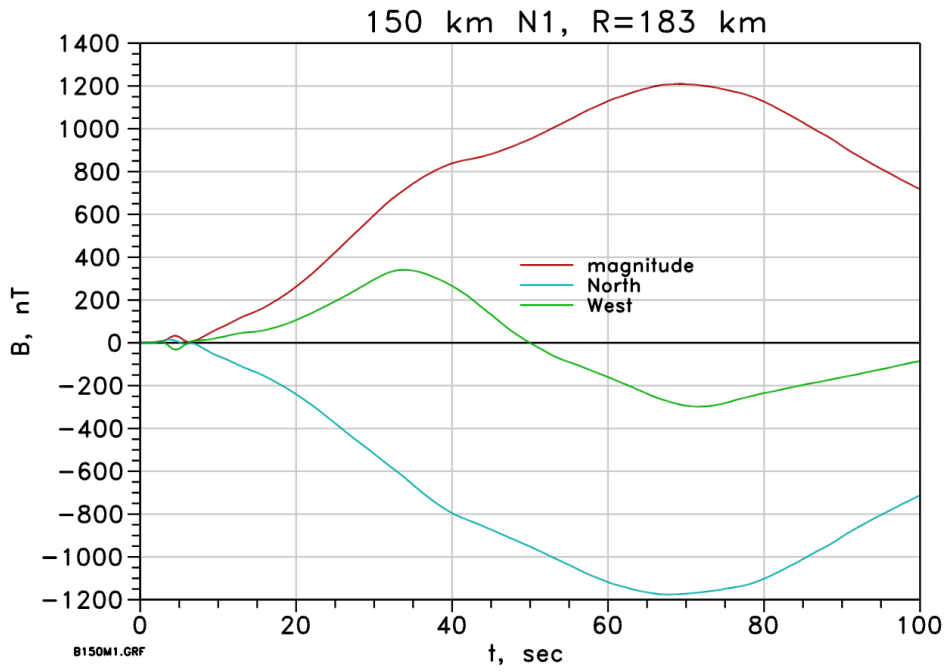


Figure 9 Measured B fields at N1, 150 km test.

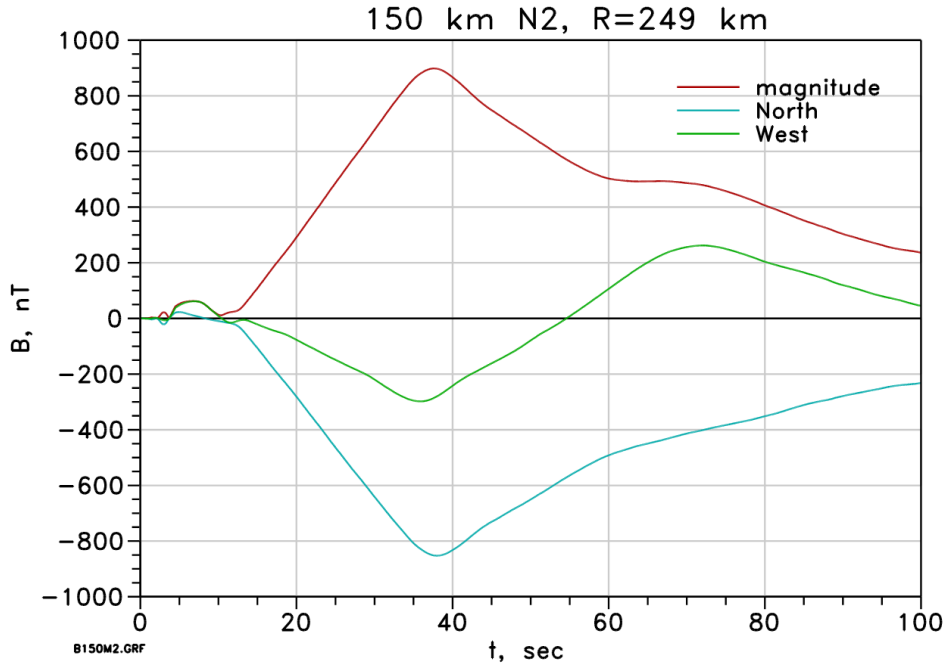


Figure 10 Measured B fields at N2, 150 km test.

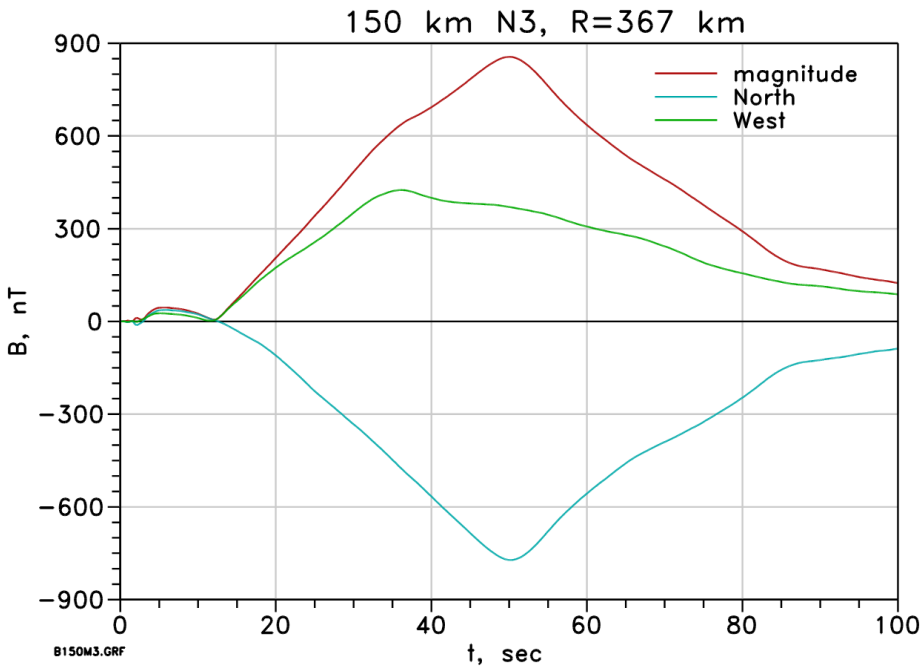


Figure 11 Measured B fields at N3, 150 km test.

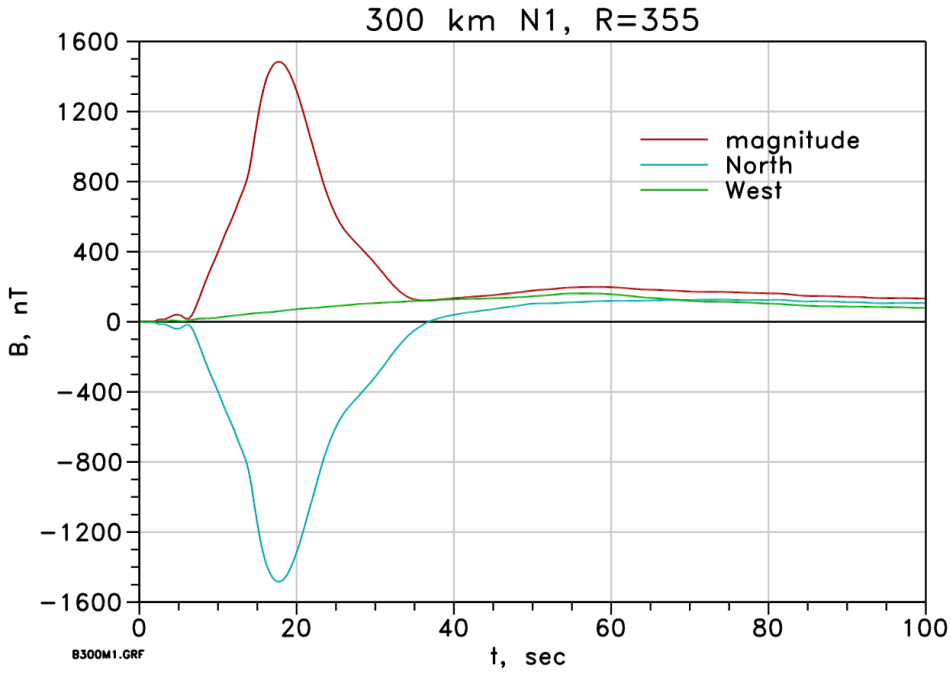


Figure 12 Measured B fields at N1, 300 km test.

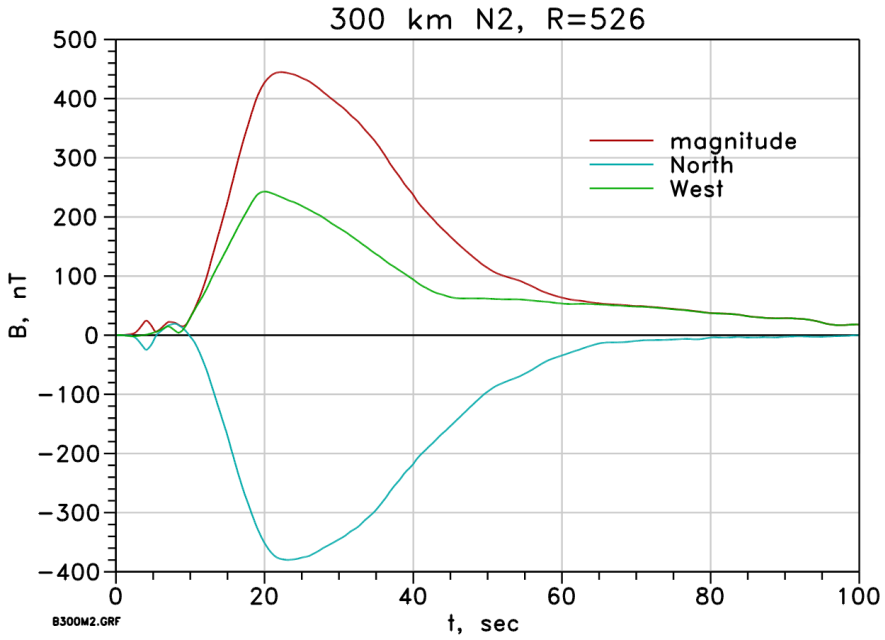


Figure 13 Measured B fields at N2, 300 km test.

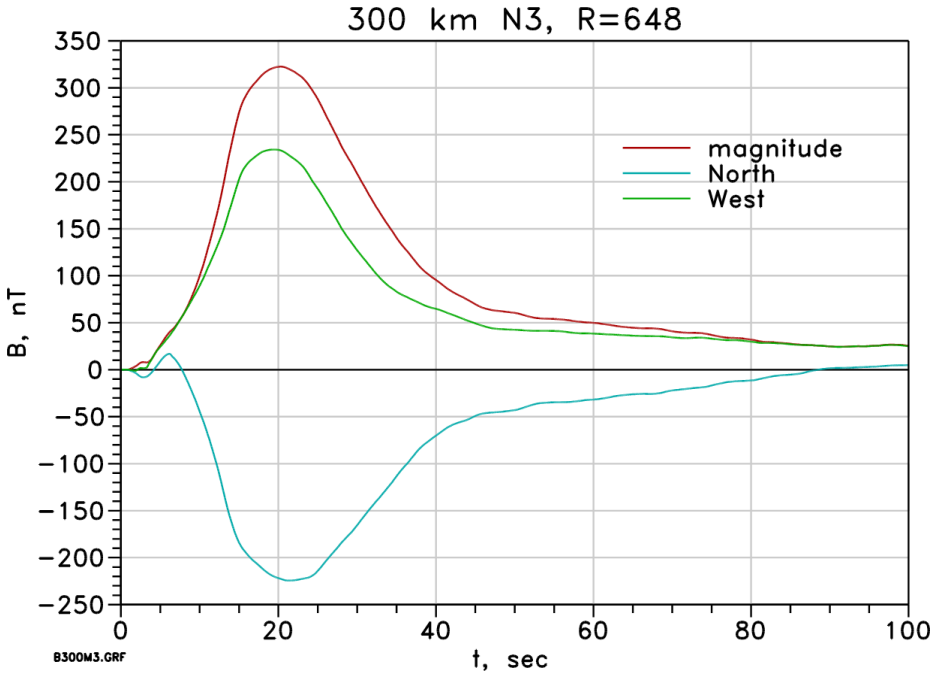


Figure 14 Measured B fields at N3, 300 km test.

The electric fields are now calculated from the measured B fields, given in nanoTeslas (nT). Table 2 lists the peak values for the calculated E fields, along with the peak values for the measured B and B-dot. The time derivative of B is often a good proxy for the behavior of the peak value of the electric field for a given ground conductivity profile. That is to say that for a given profile increases in the time derivative of the B field result in higher peak electric fields. It is noted, however, that the rest of the computed time waveform of the electric field depends more on the shape of the impedance curve and using the time derivative of the B field to compute the entire electric field waveform will not result in an accurate E field waveform.

For the following plots the measured B field components were individually computed for four sample ground profiles (a fourth severe ground profile and impedance curve was added to the previous set of three), and the resulting E field magnitudes are plotted (the total horizontal electric field is calculated by separately calculating the electric fields from the two orthogonal B field components). The 150 km cases are presented in Figure 15 to Figure 17, and the 300 km cases are presented in Figure 18 to Figure 20. These show that E fields are similar for the three ground profiles described in Figure 6. Further, the dark blue line shows the E field for a ground profile that has a very low conductivity. This profile was developed for southern Sweden and has also been used for a limited region in the northeastern United States, but it has not been used to develop the E3 HEMP results here. It is presented only to indicate that large electric fields are possible in some locations.

The highest computed E fields are for the N1 observer for the 300 km burst case. This had the highest measured B fields, and also had the narrowest time waveform—the computed peak E fields are driven higher by the enhanced time derivative of the B.

Table 2 Peaks of the Soviet measurement waveforms. (The E field is for the 10^{-3} S/m ground.)

Measurement Peaks

Burst	Observer	Peaks		
		B, nT	Ḃ, nT/min	E, V/km
R2 150 km	N1	1208.99	2141.2	4.885
	N2	898.27	3526.3	5.580
	N3	856.08	2240.2	4.241
R1 300 km	N1	1484.05	17581.4	16.585
	N2	444.69	3064.8	4.110
	N3	322.57	2642.9	3.113

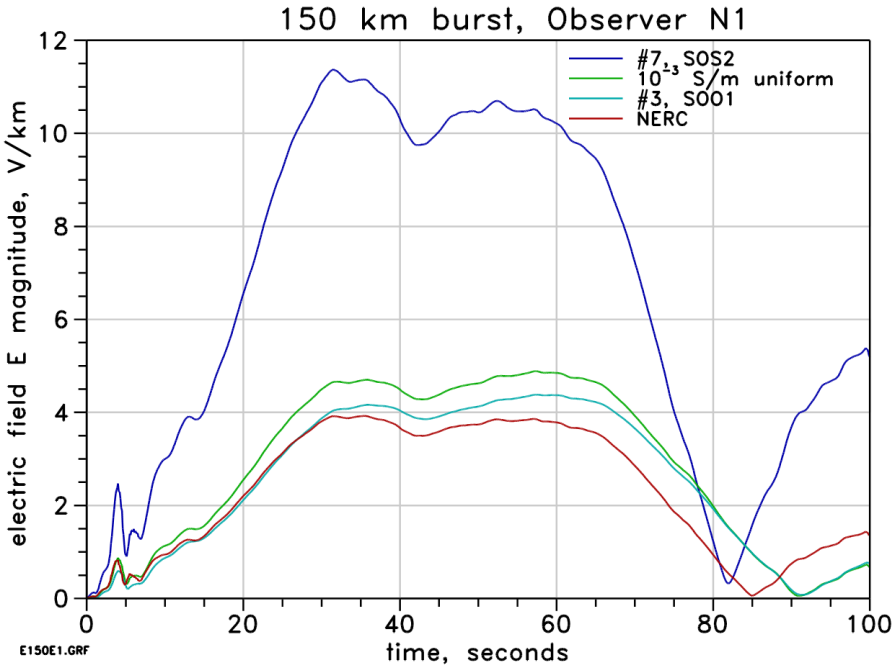


Figure 15 E field amplitudes for four ground profiles, at N1, 150 km test.

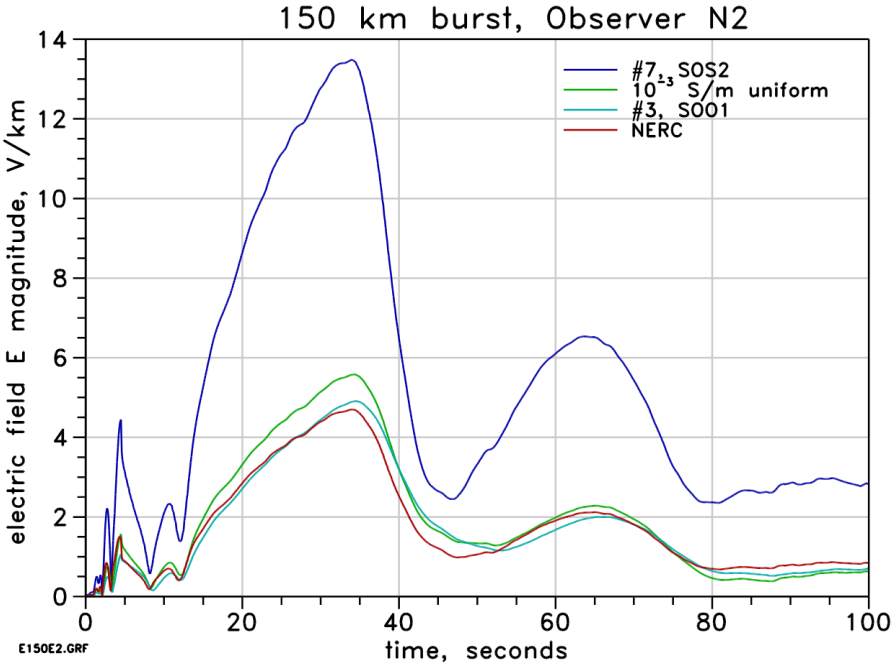


Figure 16 E field amplitudes for four ground profiles, at N2, 150 km test.

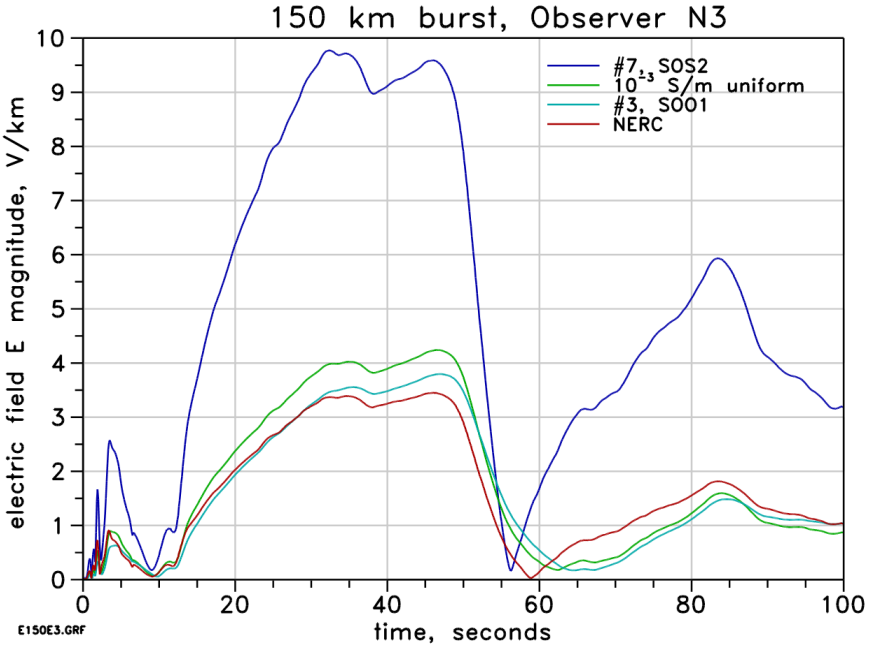


Figure 17 E field amplitudes for four ground profiles, at N3, 150 km test.

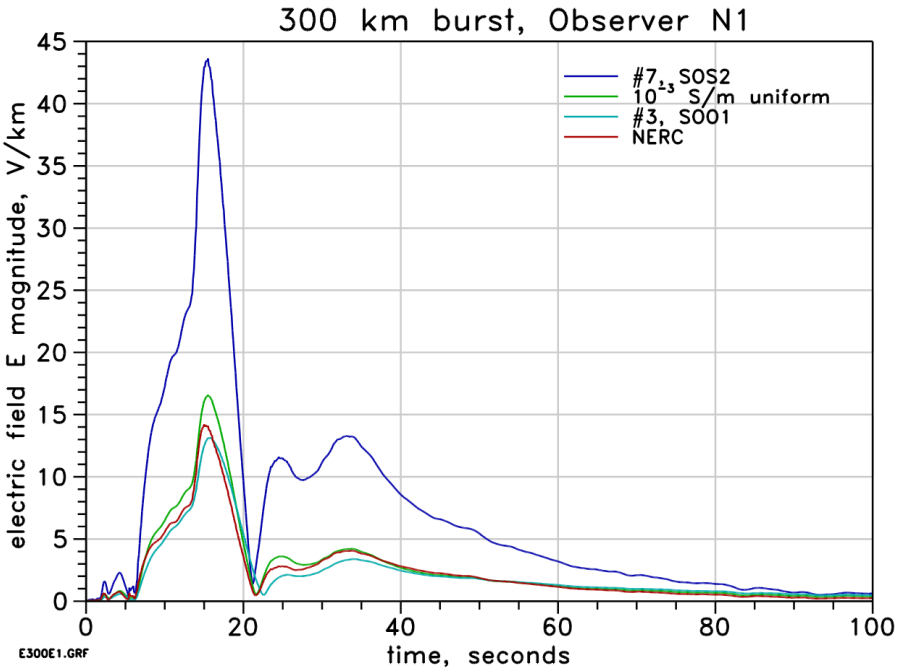


Figure 18 E field amplitudes for four ground profiles, at N1, 300 km test.

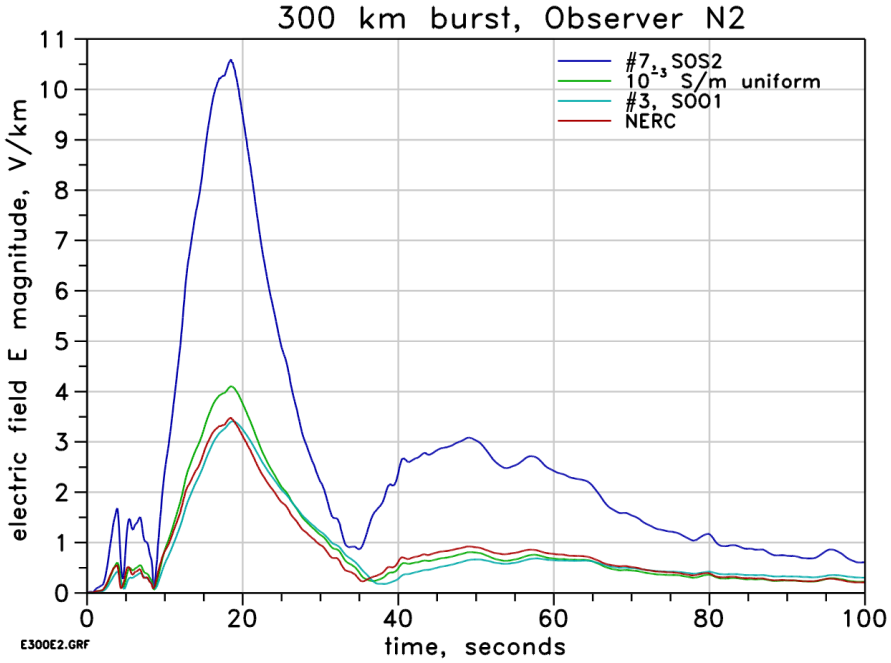


Figure 19 E field amplitudes for four ground profiles, at N2, 300 km test.

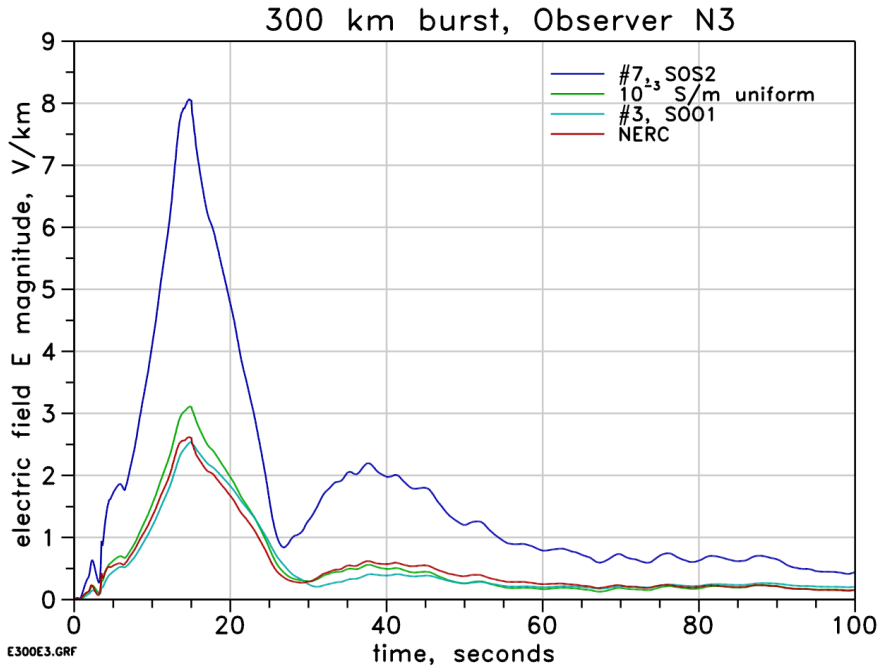


Figure 20 E field amplitudes for four ground profiles, at N3, 300 km test.

SCALING OF THE RESULTS

Even at this date the calculational models of E3 HEMP heave are not considered to be perfect, and therefore measurements are the most believable evidence of possible E3 HEMP heave field levels. However, it is extremely unlikely that even these few high-quality measurements captured the highest peak fields. Of course other test devices, especially with higher yields, could have produced higher fields, and there can be vast variations in the atmosphere conditions. For this report, the parameters of interest are the locations of the measurement observers and of the burst itself. Specific parameters are the impacts due to the geomagnetic latitude of the bursts, and whether a better location exists to place measurement sites relative to each burst. The first question is: how much higher could the measured fields have been if the burst location were closer to the geomagnetic equator? The second question is because the fields were measured at only three locations, none of which were likely to have been at the optimum point, can the measurements be scaled to the optimum point?

LATITUDE SCALING

The first consideration is the geomagnetic latitude. The geomagnetic latitude values for the two cases are found from the given physical locations:

150 km: 48.92° N
300 km: 46.13° N

These values depend on knowing the burst locations, for which there is some uncertainty, but the precise values were likely within a few degrees of these values. As discussed, the maximum peak magnetic fields increase for lower geomagnetic latitudes per the basic models.

Considering the 150 km burst case, Figure 21 shows the equivalent locations for the continental U.S. The marked red lines show geomagnetic latitude lines, and there is a black line for the 48.92°N magnetic latitude corresponding to the 150 km HOB Soviet test. If the burst had been placed anywhere along this line, the maximum peak B fields would have been as in the Soviet test. For bursts below (south) this black line, the fields would be higher.

The map shows that Texas and Florida can be as low as 35°N geomagnetic latitude. The simulation code used to perform the calculations was the same as used for the simulations shown in Figure 7 and Figure 8, but with the burst moved to lower geomagnetic latitudes—specifically the cases of 35°N that correspond to the southern points for Florida and Texas, and also for the highest levels worldwide (the geomagnetic equator). Next, the ratios of the maximum B fields from these simulations at other latitudes were compared to the maximum values for the Soviet measurement location, to get the results shown in Table 3. Using these ratio values, the Soviet measurements (“Soviet” column) were scaled to the corresponding maxima for the other latitude burst locations.

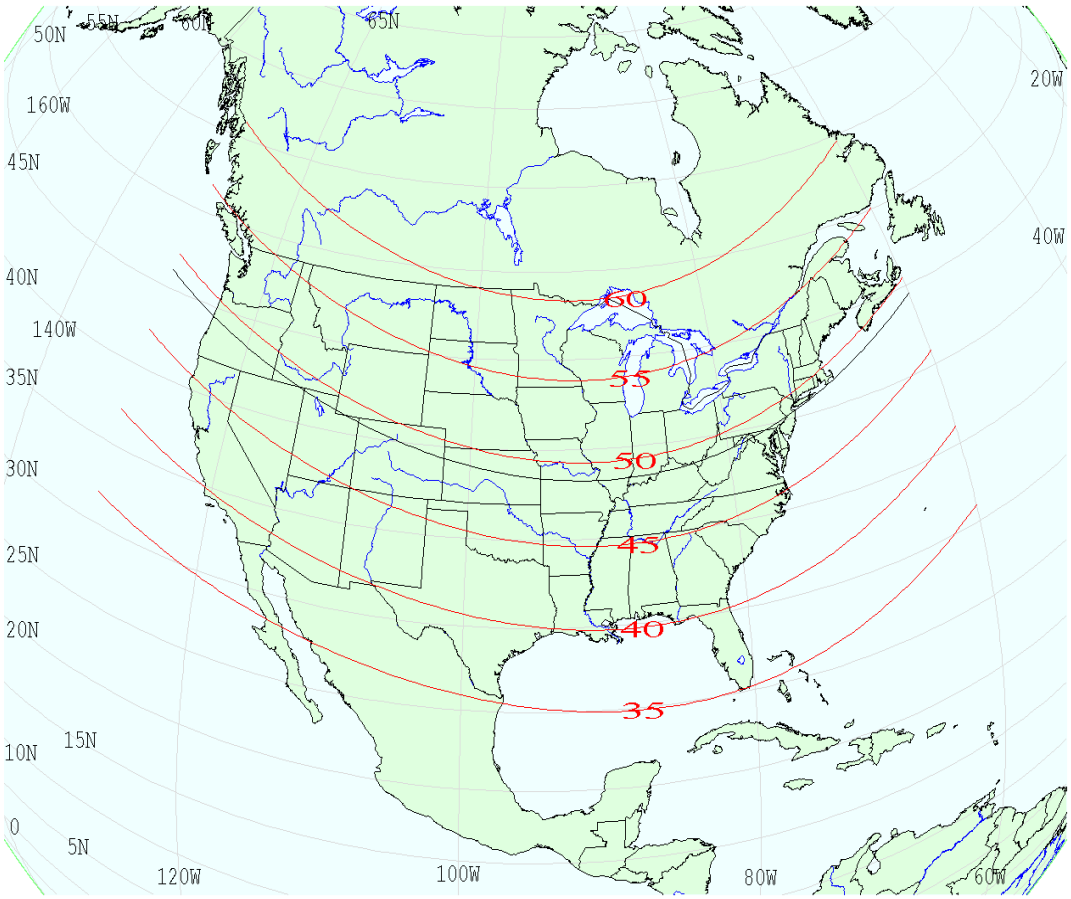


Figure 21 Geomagnetic latitude variation, for a 150 km burst, over the U.S. The black line is at 48.92º, which is the computed geomagnetic latitude for the 150 km Soviet test.

Locations outside of the continental U.S. include both lower and higher geomagnetic latitudes. The table therefore includes scaling for a magnetic latitude of 22º N, which is appropriate for Oahu, Hawaii, and also for a magnetic latitude of 65º N, as would apply to Fort Greely, Alaska.

PATTERN SCALING

The burst locations were different for the two tests, but the three observer locations stayed the same for the two tests. There is some uncertainty, however, in both the burst points and observer points. However, it is likely that the fields were higher at locations other than the three places that happened to be selected for the measurement sites. Here some understanding is sought for how high the measured fields might have been if there was a measurement at the optimal location. Figure 7 (the 150 km case), for example, shows that for this HOB the maximum is close to being directly under the burst, but the measurement sites were further out.

Table 3 Geomagnetic latitude scaling of the Soviet measurements.

Scaling of Measurements to Other Magnetic Latitudes

Burst (km)	Observer	Burst Locations							
		Soviet, B, nT	Alaska, 65° N		U.S., 35° N		Hawaii, 22° N	
			Scaling factor	B, nT	Scaling factor	B, nT	Scaling factor	B, nT
R2 150	N1	1208.99	0.600	725.28	1.364	1648.65	1.675	2025.50
	N2	898.27		538.88		1224.93		1504.93
	N3	856.08		513.56		1167.40		1434.24
R1 300	N1	1484.05	0.577	855.62	1.274	1890.47	1.537	2280.36
	N2	444.69		256.38		566.47		683.29
	N3	322.57		185.98		410.91		495.66

As noted, there is some uncertainty in the modeling and for the model parameters to use to simulate the Soviet tests. Good confidence exists, however, in the values for the ranges to the measurement sites. With this in mind, the simulation shown in Figure 22 performs E3 HEMP heave calculations at points on a 2D polar mesh; for each range of this mesh all the azimuth angles were searched to obtain three norm values: maximum, average, and minimum. The overall maximum was identified and the three norm values were normalized to this maximum value, to obtain the three lines in the plot.

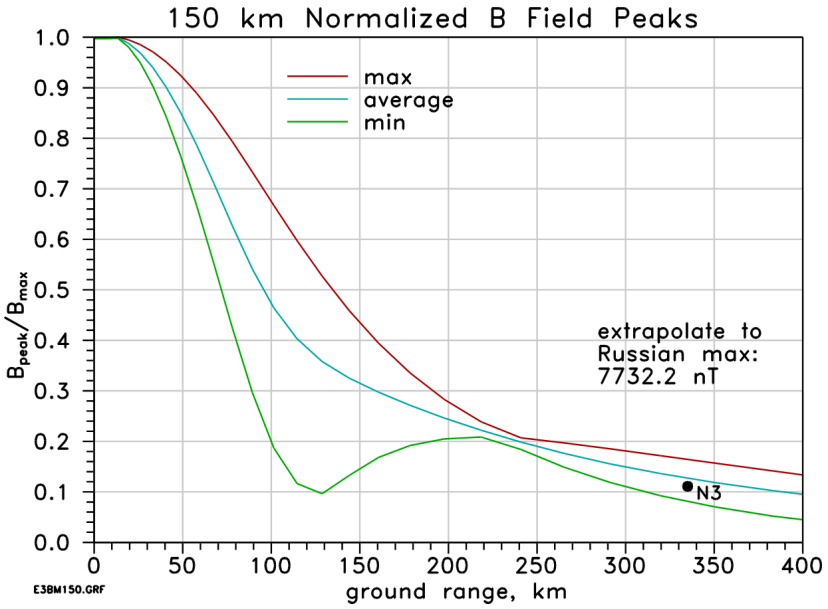


Figure 22 Normalized simulated B field peaks versus ground range for the 150 km test. The black dot

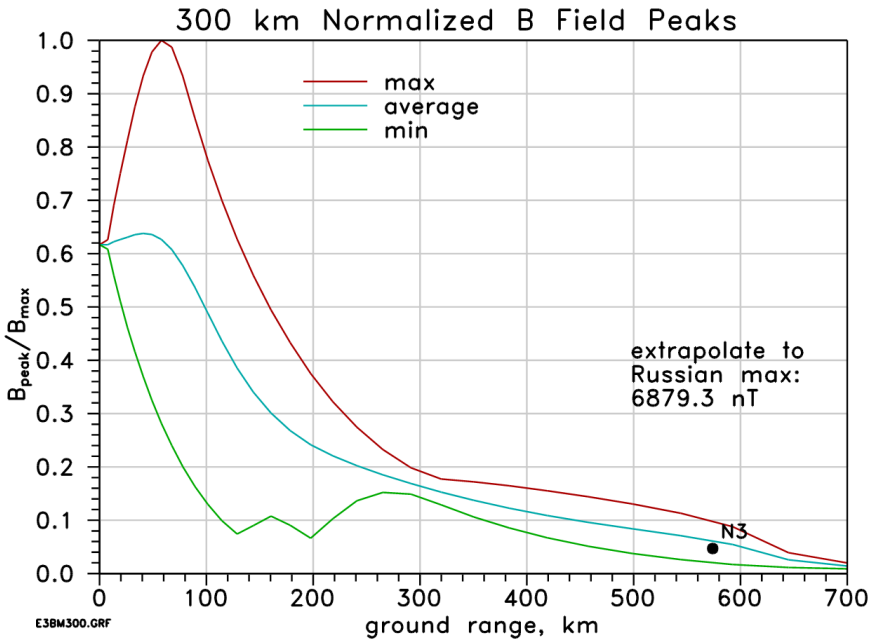


Figure 23 Normalized simulated B field peaks versus ground range for the 300 km test. The black dot shows the simulated results for the N3 point.

As noted, the precise observer azimuth positions are unknown, but the normalized value for the assumed position of the N3 observer is shown (the black dot) using a best-estimate location. Note that at this range there is not as much structure to the azimuth variation as there is closer in, such as at the 120 km range, so there is less uncertainty associated with the exact azimuth position for N3. Another way of stating this is to observe that the contour pattern becomes more circular as the observer is further away from surface zero. Using this pattern, the estimate for the maximum is then given by scaling with the factor of 9.03 (1/0.111) from the N3 point to the optimum position. The same method was used for the 300 km burst height, in the plot shown in Figure 23.

Table 4 summarizes the scaling for the two cases. The scaled values are listed in the last column. These are found by multiplying the N3 measurements (the 3rd column) by the scaling

Table 4 Pattern (observer position) scaling of the Soviet measurements.

Scaling from N3 up to the Maximum Point

Case	Soviet Measurements		Scaling	
	N1, B (nT)	N3, B (nT)	Scaling Factor	Max, B (nT)
R2, 150 km	1209.0	856.08	9.03	7732.2
R1, 300 km	1484.0	322.57	21.33	6879.3

factors (4th column, given by the reciprocal of the N3 values in Figure 22 and Figure 23). For comparison, the maximum measured values are listed in the 2nd column (the N1 points). The fact that these are smaller than the scaled maximum values is an indication that none of the observer points were very close to the optimum position.

4 CONCLUSIONS

The Soviet measurements of the E3 HEMP heave B fields were converted to E fields for a reasonable bounding case of a uniform ground conductivity of 1 mS/m. None of the three measurement points of the E3 HEMP heave fields were near the maximum in the expected field pattern, and column 3 in Table 5 gives estimates of the scaling of the measurements to the expected maximum. The three right columns provide the scaling for magnetic latitude to Hawaii, the southern portion of the continental United States, and Alaska.

Table 5 Scaling of the Soviet Measurements.

Scaling from N3 up to the Maximum Point, for Three Latitudes for 10^{-3} S/m

	Soviet Measurements		Latitude Scaling, E, V/km		
Case	Latitude (N)	E, V/km	22° N	35° N	65° N
R2, 150 km	48.92°	38.31	64.18	52.24	22.98
R1, 300 km	49.10°	66.39	102.02	84.57	38.28

Figure 24 provides a normalized waveform for one of the E fields. The electric field waveform can be used when computing the induced currents flowing in power lines, for example, to determine the amount of heating in transformer hot spots, as the time dependence of the currents are important in determining thermal effects. Figure 25 provides a sample normalized ground pattern, showing the spatial fall-off from the maximum value. Note that

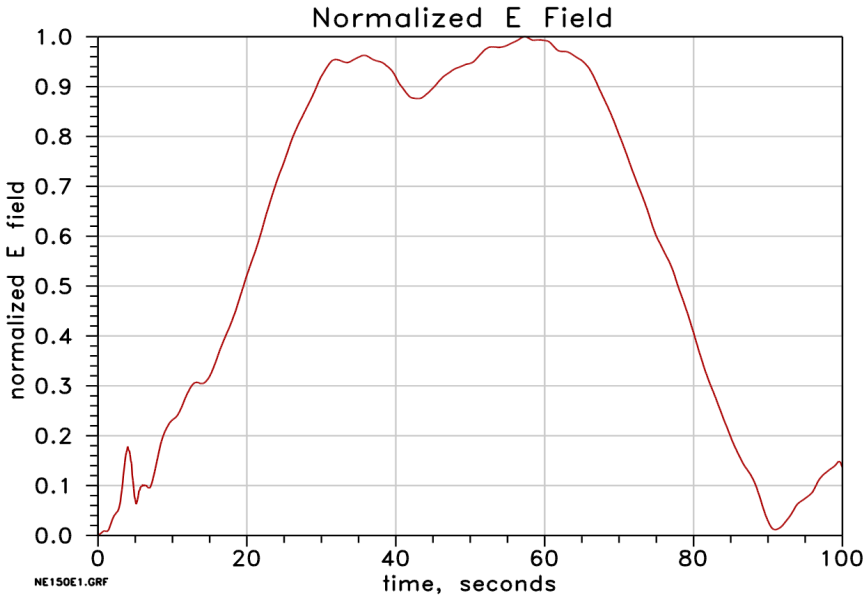


Figure 24 E field waveform shape, using the measured N1 waveform from the 150 km burst height

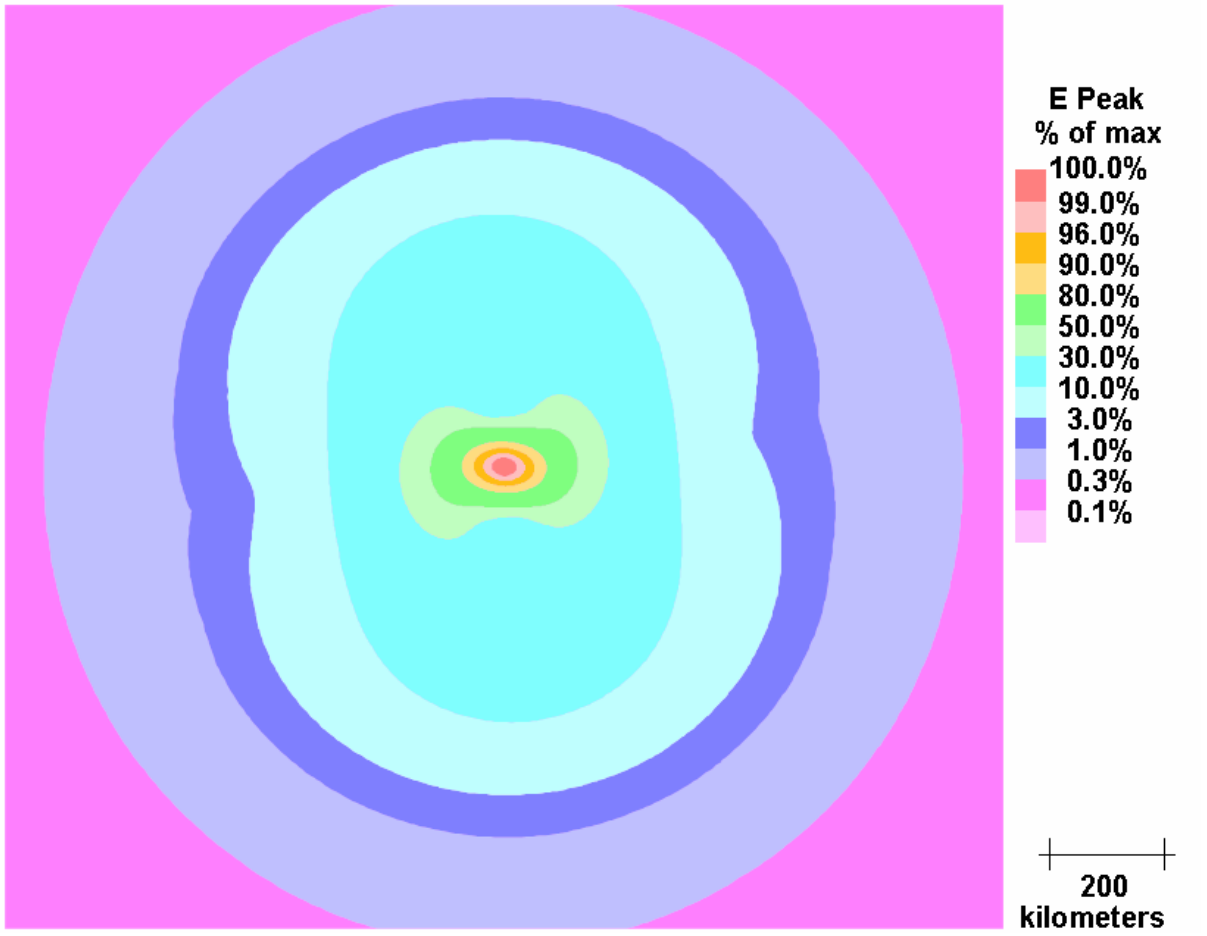


Figure 25 Normalized E peak contour pattern from the 150 km burst case

higher yield bursts could lead to even higher maximum fields, although as shown in the generic curve in Figure 3, the peak value tends to saturate as yields increase. However, this is not true for area coverage, as increasing to larger yields can increase the spatial extent of the high field region.